Journal of ELECTRONIC MATERIALS, Vol. 46, No. 10, 2017
DOI: 10.1007/s11664-017-5598-2

Further Investigation and Analysis on the Origin of the Optical Properties of Visible Hetero-photocatalyst TiO_2/CuO

NGUYEN CAO KHANG[1,2,3]

1.—Duy Tan University, 182 Nguyen Van Linh, Thanh Khe, Danang, Vietnam. 2.—Hanoi National University of Education, 136 Xuan Thuy, Cau Giay, Hanoi, Vietnam. 3.—e-mail: khangnc@hnue.edu.vn

Hetero-photocatalysts TiO_2/CuO were prepared by a wet impregnation process and their optical properties were characterized with a variety of techniques. The x-ray diffraction patterns corresponding to the anatase and the rutile phases of TiO_2 were noticed for all the samples, but the peaks belonging to CuO crystals were observed only for samples with high CuO content (≥4 wt.%). The UV–Vis spectra show that absorption edges of the modified TiO_2 were shifted toward longer wavelengths, indicating a reduction in the energy bandgap upon CuO. For photocatalytic application, the addition of CuO into TiO_2 was found to increase the photodegradation of methylene blue and methylene orange with the highest photodegradation observed at CuO content of 3 wt.%. Moreover, using some extra experimental processes, we reveal how the CuO component affects the optical properties of the resulting materials.

Key words: TiO_2, CuO, hetero-structure, photocatalysis

INTRODUCTION

TiO_2 as a photocatalyst has been extensively studied and widely applied due to its relatively high photocatalytic activity, biological and chemical stability, low cost, nontoxicity, and long-term stability against photo-corrosion and chemical corrosion.[1–3] However, the large bandgap of TiO_2 (3.2 for the anatase phase and 3.0 eV for the rutile phase) limits the light interaction only to UV light which accounts for 4% of the solar spectrum. Of many approaches to extend the spectral response to the visible light region, doping (metal and nonmetal) has been considered as the most effective.[4,5] However, in metal-doped or nonmetal-doped TiO_2, it is difficult to control nonmetal doping concentration, or to avoid the formation metal oxide clusters. Consequently, the composite materials developed from such original photocatalysis have been more attractive objects in photocatalysis research and application.

(Received December 28, 2016; accepted May 16, 2017; published online May 31, 2017)

Among these modified photocatalysts, TiO_2/CuO hetero-structures have been of great interest thanks to their well-performing visible photoactivities and simple preparations.[6,7] TiO_2/CuO nano-structures with a narrower energy band gap have been synthesized, using various preparation techniques, including wet chemical processing,[8,9] hydrolysis,[10] and electrospinning.[11] Bandara and Choi reported that hydrogen production of pure TiO_2 was markedly enhanced by CuO compositing.[12,13] Wu et al.[14] has developed TiO_2/CuO composite nanoparticles for H_2 generation and reported significant enhancement of photocatalytic H_2 generation compared with that of TiO_2/Pt of about 10%. Xu et al.[15] investigated TiO_2 with deposited Cu, and found that this sample had high efficiency for reaction photocatalytic application. Many studies have focused on the photocatalytic application of TiO_2/CuO. However, the optical properties of such modified photocatalyts, especially the original mechanism of band gap reduction on these properties, have not been properly investigated.

In the present work, a series of TiO_2/CuO nano hetero-structures was prepared by a wet impregnation process using precursors TiO_2 P25 and Cu(II)

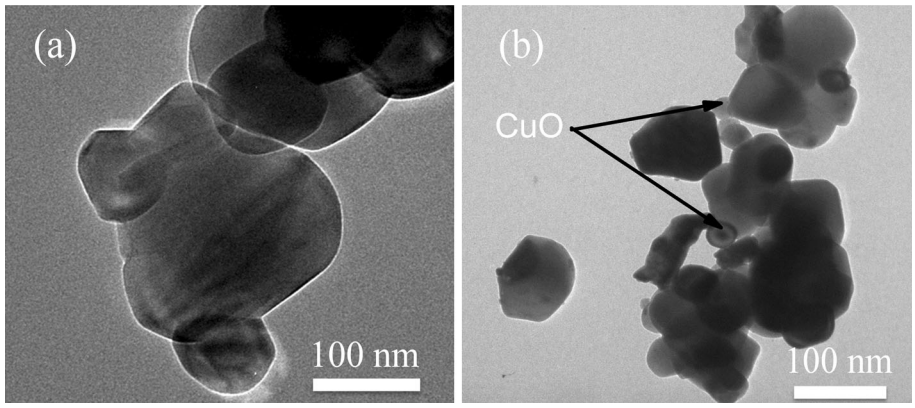

Fig. 1. TEM images of the (a) pure TiO_2, and (b) TiO_2/CuO contents at 3%.

salt. We focally analyzed the modifications based on the optical property of the photocatalysts as well as their mechanisms based on UV–Vis reflective diffusive spectra measurements. Moreover, by developing some extra experimental processes, we have evaluated the role of CuO, of Cu^{2+} ions attached to TiO_2 in the variation of the optical property of the resulting materials.

SYNTHESIS AND CHARACTERIZATION

TiO_2 P25 powders and $Cu(NO_3)_2{\cdot}3H_2O$ were magnetically stirred in iso-propanol for 4 h at 95°C and entirely dried at room temperature. The obtained residue was ground for 4 h and then heated at 500°C for 2 h. By changing the amount of initial supports, a series of TiO_2/CuO samples with various CuO wt.% was prepared. For a deeper understanding of the role of CuO in reducing the bandgap, CuO was then removed from the TiO_2/CuO sample by HNO_3 acid.

Transmission electron microscopy (TEM) analysis was performed using a transmission electron microscope (JEOL 1200CX) with an accelerating voltage of 80 kV. The structure of the TiO_2 samples were determined by x-ray diffractometer D5005 (Siemen) with CuKα radiation (λ = 1.5406 Å). The element composition was confirmed by energy dispersive x-ray (EDX) spectroscopy analysis. Optical absorption spectra were measured by V-670 spectrophotometer. The photocatalytic efficiency of the resulting samples was evaluated through the decomposition of methylene blue (MB) and methylene orange (MO) dyes under visible light. The self-designed reactor vessels containing 200 mL of dyes solution (10 ppm) mixed with 100 mg of photocatalyst powders were placed under visible radiation. The temperature stabilization and magnetically stirring system were equipped for maintaining the homogeneous and unique conditions for all tests. An optical system with a 400 nm filter in front of a 150 W Xenon lamp L2273 was used as the visible radiation source. Before turning on the light, the suspension containing the dyes and the photocatalyst were

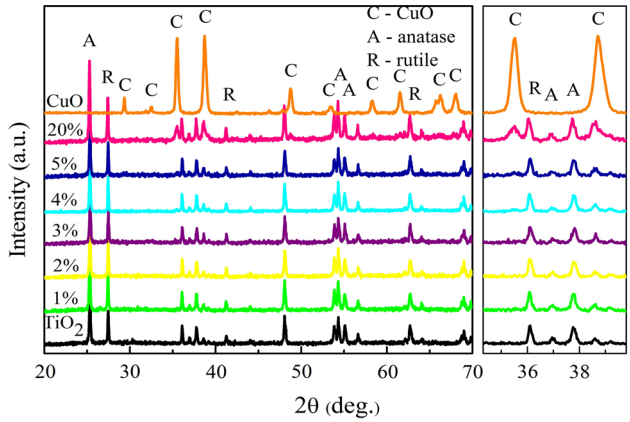

Fig. 2. X-ray diffraction patters of TiO_2, CuO, and TiO_2/CuO with various CuO contents.

magnetically stirred continuously in the dark until no change in the absorbance of the solution was observed. The purpose of this process was to make sure that the physical adsorption plays no role in reducing the dye concentration. Additionally, the dye solution without a catalyst illuminated in the same conditions for 4 h to investigate the decomposition of dyes by light source was used as a control sample. The reduction in the concentration of the dyes was determined by monitoring UV–Vis spectra.

RESULTS

TEM was used to study the size and shape of the samples. Shown in Fig. 1 are TEM images of TiO_2 P25 sample (Fig. 1a) and TiO_2/CuO with 3 wt.% CuO (Fig. 1b). It can be seen that the shapes of the particles are completely spherical, and relatively monodispersed. The size of TiO_2 is uneven, ranging from 70 nm to 200 nm. CuO particles which are located on the surface of TiO_2 have a size of about 20 nm, indicated by arrows as shown in Fig. 1b.

Powder x-ray diffraction (XRD) was carried out to study the crystallographic structure of the materials. The XRD patterns in Fig. 2 exhibit

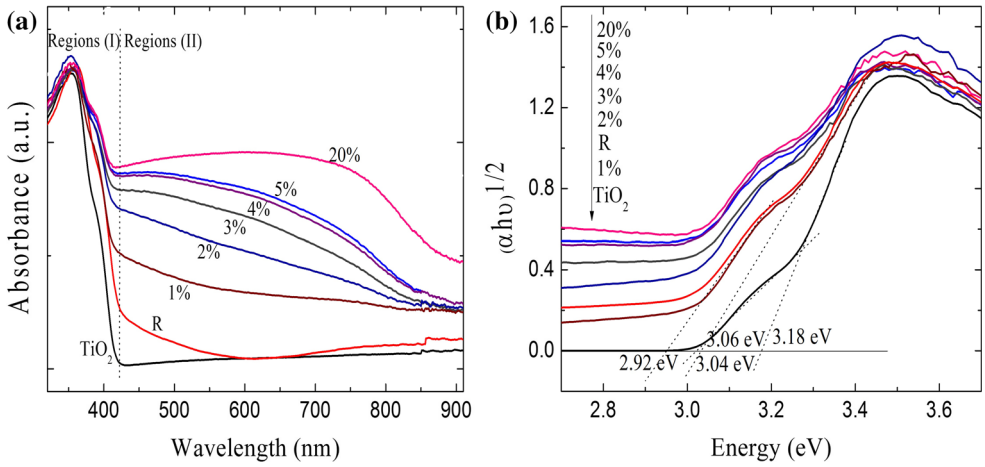

Fig. 3. (a) UV–Vis diffusive reflective spectra of TiO_2, and TiO_2/CuO with various CuO contents: 1, 2, 3, 4, 5, and 20%; (b) the transformed Kubelka–Munk function versus energy of the excitation source.

Table I. The energy band gap values of the samples

TiO_2/CuO samples	Pure TiO_2	CuO-removed sample (R)	1% CuO	2% CuO	3% CuO	4% CuO	5% CuO	20% CuO
E_g (eV)	3.18	2.98	2.96	2.91	2.84	2.85	2.85	2.83

characteristic peaks of the anatase (~79%) and rutile phases of TiO_2 (~21%). The location, shape, and relative intensity of these peaks remain unchanged, indicating no influence of CuO on the structure of the TiO_2. The peaks at 2θ of 35.6° and 38.7° belong to CuO crystals and can be observed only for samples with high CuO concentration (≥4 wt.% in the present work). Conventionally, metal oxide doping (such as Al_2O_3, NiO, CeO_2, ZrO_2 and Sb_2O_5) is used to extend the anatase to the rutile transformation to a higher temperature (700°C).[16–18] However, some metal oxides like Li_2O, ZnO, MgO and Sb_2O_3 accelerate this transformation.[19,20] The results in Fig. 2 show that the intensities of the peaks at 25.5° and 27.5° slightly increase with increasing the CuO content, implying the influence of CuO on the crystallization of TiO_2. However, the intensity ratio of these two peaks is nearly unchanged in the TiO_2/CuO samples, indicating that CuO has almost no influence on the anatase phase to the rutile phase transformation.

To investigate the optical properties of the TiO_2/CuO composite materials, the UV–Vis spectra were recorded and are shown in Fig. 3a. It can be seen that the enhancement of visible absorption of TiO_2 upon CuO doping is remarkably different from that of supporting TiO_2. All TiO_2/CuO samples contain two interesting features: the first (region I) is characterized by an absorption edge extending to above 400 nm and the second (region II) is featured by its broadness ranging from 550 nm to 900 nm (see Fig. 3a). The fact that the two distinguishable absorption edges corresponding to the anatase and the rutile phases were shifted toward longer wavelengths is consistent with a reduction in the band gap E_g of CuO upon doping, as observed in Fig. 3b. The figure clearly shows a decrease in E_g from 3.18 to 2.84 eV for the anatase phase and from 3.02 to 2.83 eV for the rutile phase when the CuO concentration increases from 1 wt.% to 4 wt.%. Interestingly enough, the change in E_g is no longer observed after the CuO content reaches 4 wt.%. The results of calculation of band gap energy of all the samples are listed in Table I.

Previous literature[21,22] has attributed the first absorption (between 380 nm and 420 nm) to the interfacial charge transfer from the O2*p* valence band to the Cu(II) state which can be presented by Cu^{2+} ions attached to TiO_2 (Cu(II) cluster). On the other side, the second absorption band (between 550 nm and 900 nm) was assigned to the *d–d* transition of Cu^{2+} in the crystalline environment of TiO_2.[23] In this article, the treatment temperature of the samples is 400°C, making it possible for some of the Cu^{2+} ions to replace surface Ti^{4+} sites.

For a better understanding of the influences of CuO on E_g, the TiO_2/CuO with 20 wt.% CuO samples were washed with HNO_3 acid several times to remove CuO on the material (CuO-removed sample). It can be expected that the Cu^{2+} attached to TiO_2 (in form of Cu(II) clusters) will not be influenced by this treatment. An absorption spectrum of a treated sample (the red line in Fig. 4a) shows that the extra visible absorption region from

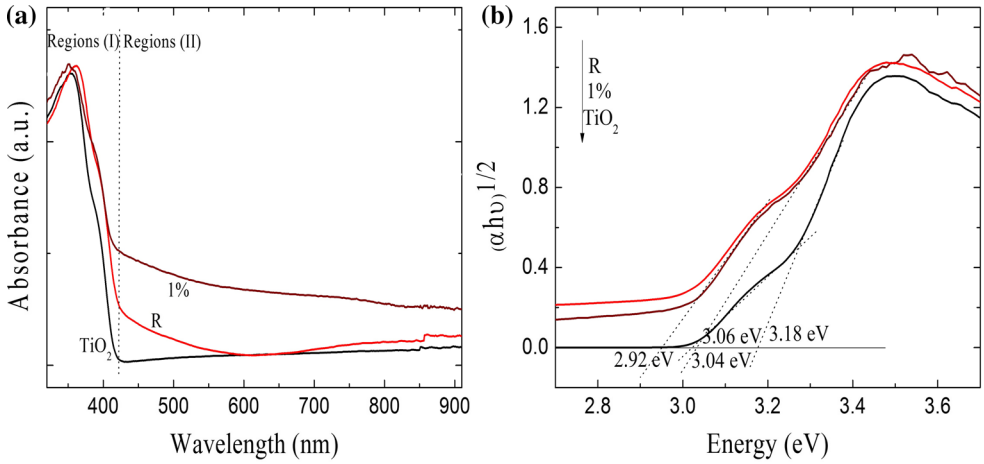

Fig. 4. (a) UV–Vis diffusive reflective spectra of the sample CuO-removed (R), pure TiO_2, and TiO_2/CuO with CuO contents at 1%; (b) the transformed Kubelka–Munk function versus energy of the excitation source.

500 nm to 900 nm is no longer present. This suggests that it is not the Cu(II) clusters but the CuO locating in TiO_2 lattice which accounts for the 550–900 nm band. However, the treated sample still performs a red shift in the absorption region from 380 nm to 420 nm. This red shift in the absorption edge of TiO_2 was still observed, but with a shift less visible than those of the untreated samples. This indicates that CuO has little effect on E_g or, in other words, the change in E_g observed in the treated sample can be mainly attributed to the Cu(II) clusters. So, the presence of Cu(II) clusters (they are not washed by acid) is the reason for the small visible-shifting in the absorption spectrum of the treated sample. This is consistent with what Li et al.[23] suggested: the 380–420 nm absorption band was mainly due to the charge transition from the valence band of TiO_2 to the Cu^{2+} attached to TiO_2 (Cu(II) clusters).

For the elemental microanalysis of TiO_2/CuO (20 wt.% CuO) and CuO-removed samples, EDX spectra were used. Figure 5 shows the EDX spectra of TiO_2/CuO and CuO-removed samples. Peaks belonging to Cu are present in both spectra. However, the Cu peak of the TiO_2/CuO sample is much more intense than that of the CuO-removed sample. The quantitative elemental contents of the samples are compiled in Table II. The percent of Cu in the TiO_2/CuO (20 wt.% CuO) sample reaches 16.19%, while the amount of Cu in the CuO-removed sample is only 1.53%. This result indicates that the HNO_3 acid only removes CuO on the TiO_2/CuO material, but has no influence on the Cu^{2+} attached to TiO_2. The small amount of Cu (1.53%) corresponding to Cu^{2+} attached to TiO_2 contributes significantly to the shift in the absorption edge of TiO_2 in the 380–420 nm range, as shown on the absorption spectrum in Fig. 4.

The photocatalyst activity of the synthesized samples and the photo-degradation efficiencies of both the MB and MO dyes were studied and are shown in Fig. 6 which reveals a strong dependence of the amount of dyes decomposed on the content of CuO in the photocatalysts. The modified samples containing 3 wt.% of CuO exhibited considerably enhanced photo-efficiencies, which are approximately 4 and 2.5 times higher than that of the pure TiO_2 for the degradation of MB and MO, respectively. For the samples with CuO contents lower than this optimum range, the photo-degradation increases with increasing CuO content due to the gradual reduction in the energy band gap of these samples. In this case, the materials can absorb higher wavelengths, facilitating the electron–hole generation which in turn promotes the number of photo-degradation reactions of the organic molecules. However, for samples with a concentration of CuO 4wt.% and more, the photo-efficiency falls rapidly and even reaches a point which is less effective than the original TiO_2. This result can be explained by considering the shading effect originating from the excellent absorption behavior of the CuO particles. When the CuO content exceeds its optimum value, the CuO species tend to aggregate into larger clusters covering the TiO_2 photocatalyst particles. Consequently, the illuminated photos have been absorbed by these CuO clusters, the non-photoactive elements, before reaching and being absorbed by the photoactive TiO_2.

Figure 6 also shows the photo-degradation efficiencies by the CuO-removed sample (the sample TiO_2/CuO with 20 wt.% CuO; however, the CuO was removed by HNO_3 acid). The results indicate that the ability to decompose the dyes of this sample is worse than the TiO_2/CuO with the 20 wt.% sample, but better than the remaining samples. Thus, the red-shifting in the absorption region from 380 nm to 420 nm due to the Cu(II) clusters plays a more important role in enhancing the photocatalytic activity.

For applications, the stability of a photocatalyst is an important parameter. Here, the reliability and stability of the photocatalytics of the TiO_2/CuO with

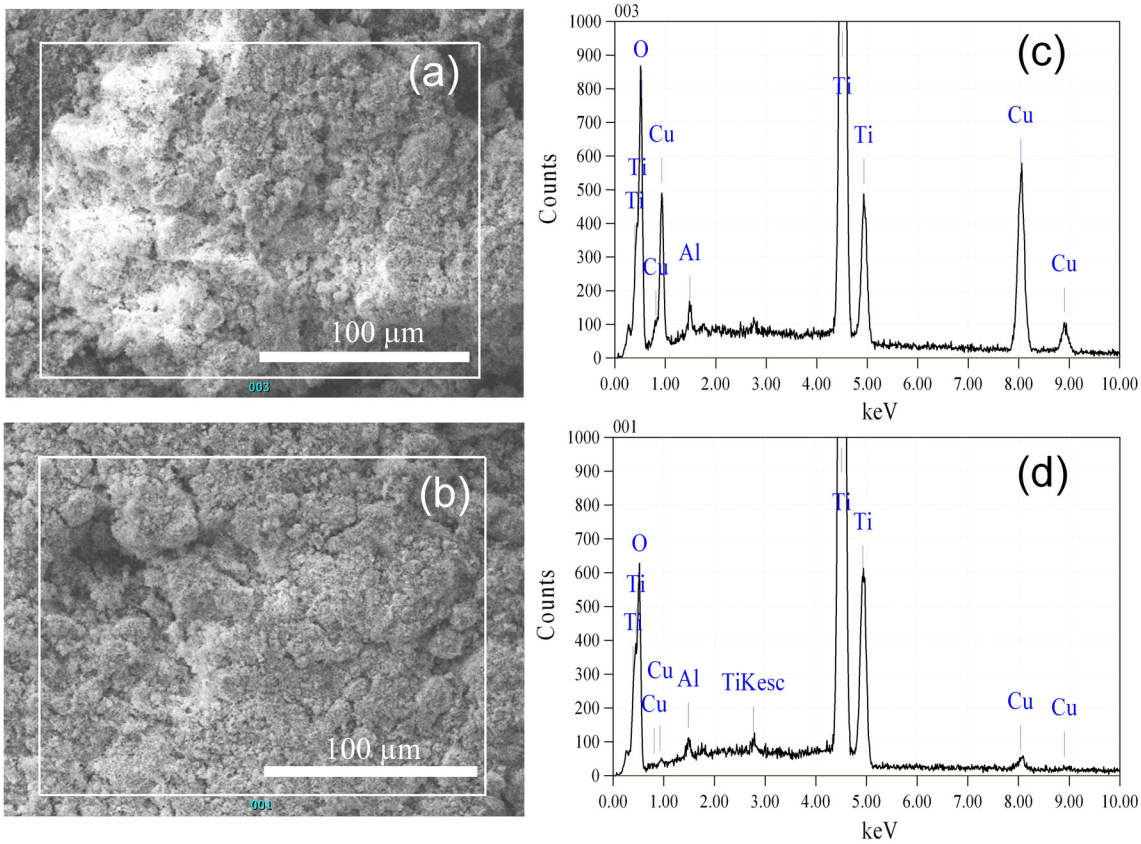

Fig. 5. (a, b) SEM-micrographs and (c, d) EDX spectra of TiO_2/CuO (20 wt.% CuO), and CuO-removed samples, respectively.

Table II. EDX analysis results of the TiO_2/CuO (20 wt.% CuO), and the CuO-removed sample

Samples	O (wt.%)	Ti (wt.%)	Cu (wt.%)	Others (wt.%)
TiO_2/CuO (CuO content 20 wt.%)	36.11	46.99	16.19	0.71
CuO-removed sample	40.33	57.78	1.53	0.36

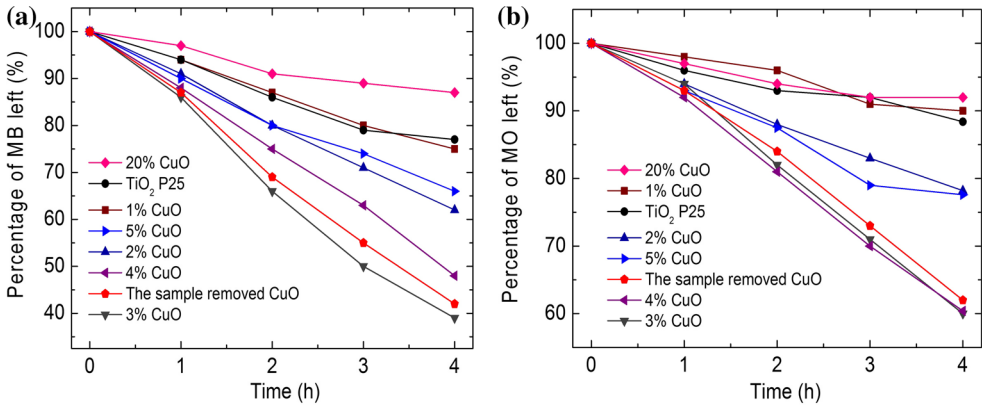

Fig. 6. Photodecomposition of (a) MB, and (b) MO catalyzed by the catalysts under visible-light illumination.

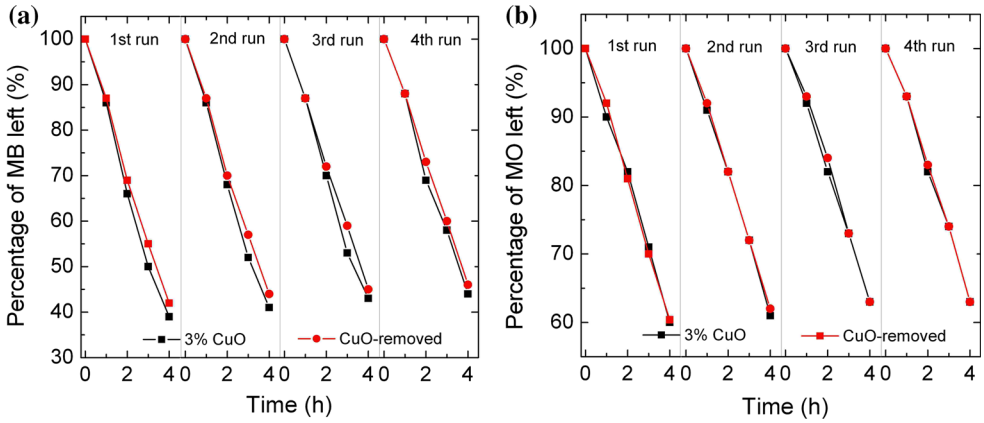

Fig. 7. Photocatalytic activities of the TiO_2/CuO with 3 wt.% CuO sample (squares) and the CuO-removed TiO_2/CuO sample (circles) for the degradation of (a) MB, and (b) MO under visible light irradiation for four cycles.

the 3 wt.% CuO sample and the CuO-removed sample were evaluated by circulating runs in the photocatalytic degradation of dyes under visible light irradiation. As shown in Fig. 7, after four successive experimental runs, the degrading of MB decreased a little bit, from 60% to 55%, for the TiO_2/CuO with the 3 wt.% CuO sample, whereas the amount degraded of MB decreased from 58% to 52% for the CuO-removed sample. The result in Fig. 7 also reveals that there is no noticeable decrease in photocatalytic activity of MO up to the fourth cycle. This result indicated that the photodegradation ability of all samples after four photocatalytic experiments was almost identical to that of the fresh samples.

CONCLUSIONS

The optical properties of various TiO_2/CuO photocatalysts obtained by the wet impregnation process were experimentally investigated and analyzed. The XRD patterns corresponding to the characterized peaks of the CuO crystals (at 35.6° and 38.7°) were observed, but only for samples with a CuO content higher than 3 wt.%. The composite material can absorb light with higher wavelengths and the absorption even covers the whole range of the visible region. The percent of MB and MO decomposed depends on the ratio between TiO_2 and CuO, and the highest decomposition rate of MB and MO on the catalysts was observed for samples with 3 wt.% of CuO. The Cu(II) clusters were mainly responsible for the red shift in the absorption edge observed in the 380–420 nm range, while the CuO located on the surface of TiO_2 accounts for the broad absorption peak from 500 nm to 900 nm. By developing some extra experimental processes, we found that an interesting result of this study is that it is not the CuO but the Cu^{2+} attached to TiO_2 component which plays a vital role in enhancing the photocatalytic properties of TiO_2/CuO materials prepared by a wet impregnation process.

ACKNOWLEDGEMENT

This work was supported by the Nafosted No. 103.02-2016.66.

REFERENCES

1. X. Chen and S.S. Mao, *Chem. Rev.* 107, 2891 (2007).
2. A. Fujishima and K. Honda, *Nature* 238, 37 (1972).
3. M.R. Hoffmann, S.T. Martin, W. Choi, and D.W. Bahnemann, *Chem. Rev.* 95, 69 (1995).
4. B. Tryba, J. Orlikowski, R.J. Wróbel, J. Przepiórski, and A.W. Morawski, *J. Mater. Eng. Perform.* 24, 1243 (2015).
5. M. Zhang, X. Yu, D. Lu, and J. Yang, *Nanoscale Res. Lett.* 8, 543 (2013).
6. D.P. Kumar, M.V. Shankar, M.M. Kumari, G. Sadanandam, B. Srinivas, and V. Durgakumari, *Chem. Commun.* 49, 9443 (2013).
7. W. Slamet, H.W. Nasution, E. Purnama, S. Kosela, and J. Gunlazuardi, *Catal. Commun.* 6, 313 (2005).
8. L.S. Yoong, F.K. Chong, and B.K. Dutta, *Energy* 34, 1652 (2009).
9. L.T. Ngoc, H.V. Thanh, N.T.H. Le, N.V. Chien, T.D. Thanh, D.H. Manh, V.D. Lam, N.X. Nghia, D.T. Hoa, L.Q. Huy, N.M. Hong, and L.V. Hong, *Adv. Nat. Sci. Nanosci. Nanotechnol.* 3, 45009 (2012).
10. S.S. Lee, H. Bai, Z. Liu, and D.D. Sun, *Water Res.* 47, 4059 (2013).
11. L. Zhu, M. Hong, and G.W. Ho, *Nano Energy* 11, 28 (2015).
12. J. Bandara, C.P.K. Udawatta, and C.S.K. Rajapakse, *Photochem. Photobiol.* 4, 857 (2005).
13. H.J. Choi and M. Kang, *Int. J. Hydrog. Energy* 32, 3841 (2007).
14. N.L. Wu and M.S. Lee, *Int. J. Hydrog. Energy* 29, 1601 (2004).
15. S. Xu and D.D. Sun, *Int. J. Hydrog. Energy* 34, 6096 (2009).
16. R.D. Shannon and J.A. Pask, *J. Am. Ceram. Soc.* 48, 391 (1965).
17. M.S.P. Francisco and V.R. Mastelaro, *Chem. Mater.* 14, 2514 (2002).
18. U. Gesenhues, *Solid State Ion.* 101, 1171 (1997).
19. U. Gesenhues, *Chem. Eng. Technol.* 24, 685 (2001).
20. B. Grzmil, B. Kic, and M. Rabe, *Chem. Pap.* 58, 410 (2004).
21. B. Choudhury, M. Dey, and A. Choudhury, *Int. Nano Lett.* 3, 1 (2013).
22. A. Di Paola, E. García-López, G. Marcìa, C. Martín, L. Palmisano, V. Rives, and A. Maria Venezia, *Appl. Catal. B Environ.* 48, 223 (2004).
23. G. Li, N.M. Dimitrijevic, L. Chen, T. Rajh, and K.A. Gray, *J. Phys. Chem. C* 112, 19040 (2008).